PASJ: Publ. Astron. Soc. Japan **51**, 587–593 (1999)

VLBA Observation of SiO Masers in the M Giant IRC −10414

Hiroshi IMAI*
Astronomical Institute, Graduate School of Science, Tohoku University, Aoba, Sendai, Miyagi 980-8578
E-mail (HI): imai@miz.nao.ac.jp

Shuji DEGUCHI
Nobeyama Radio Observatory, National Astronomical Observatory, Minamimaki, Minamisaku, Nagano 384-1305
and
Makoto MIYOSHI†
Mizusawa Astrogeodynamics Observatory, National Astronomical Observatory, Mizusawa, Iwate 023-0861

(Received 1999 January 29; accepted 1999 July 6)

Abstract

We have mapped an M giant star, IRC −10414, in the SiO $J = 1$–0 $v = 1$ line at 43.1 GHz with the VLBA‡ with a spatial resolution of better than 0.5 mas. The maser spots spread over on a circle having a radius of about 7.1 mas. A velocity gradient in the east-west direction of ~ 0.7 km s^{-1} mas^{-1} is found. Monitoring observations with Nobeyama 45-m telescope have shown that the intensity ratio of the SiO $J = 1$–0 $v = 1$ to $v = 2$ maser line was quite unusual (5–40) for the period of 1997–1999 in this object; this ratio was known to be close to unity in many late-type stellar objects, but was known to deviate strongly from unity in young stellar objects. The unusual line intensity ratio of this star may suggest a chemical or geometrical anomaly of the envelope of IRC −10414. A possible ring/disk model is discussed in order to explain the distribution of the maser spots in this object.

Key words: Infrared: sources — Masers — Radio sources: lines — Stars: circumstellar shells — Stars: individual (IRC −10414) — Stars: late-type

1. Introduction

The infrared source IRC −10414 (GL 2139, IRAS 18204−1344, or OH 17.551−0.126) is classified as a M6.5 giant (Lockwood 1985). It is a strong maser source detected by OH 1612 and 1665/1667 MHz and by H_2O and SiO (see Engels 1979; Ukita, Goldsmith 1984). The mass-loss rate of this star was estimated from the infrared spectrum as being $4 \times 10^{-6}\,M_\odot$ yr^{-1} (Jura, Kleinman 1989).

In the course of a SiO maser survey in the galactic plane with the Nobeyama 45-m telescope (Izumiura et al. 1999), we noticed that the SiO $J = 1$–0 $v = 2$ line at 42.821 GHz of IRC −10414 was quite weak and almost undetectable, although the SiO $J = 1$–0 $v = 1$ line at 43.122 GHz was strong, about $T_a = 10$ K. In normal late-type stars with SiO masers, the line intensity ratio of the $J = 1$–0 $v = 1$ to the $J = 1$–0 $v = 2$ transition is nearly unity (Shwartz et al. 1979; Spencer et al. 1981; Nakada et al. 1993). Though there had been arguments concerning the intensity ratio of these two transitions (Nyman, Olofsson 1986), the simultaneous observations of the two transitions at Nobeyama have confirmed that this ratio is about unity on average for galactic bulge stars, and that almost 90% of the sources show this ratio to be in the range of 0.5–2.0 (Jiang et al. 1995).

It is known that in young stellar objects this intensity ratio is frequently far from unity. For example, in Sgr B2 MD5 the $J = 1$–0 $v = 1$ transition had been detected, but almost no emission was found in the $J = 1$–0 $v = 2$ transition (see the profile in Shiki et al. 1997). In W51 IRS2, it is opposite; only the $J = 1$–0 $v = 2$ line has been detectable (Hasegawa et al. 1985; Fuente et al. 1989; Morita et al. 1992).

It may be suggested that the SiO line intensity ratio of the $J = 1$–0 $v = 1$ to 2 transition has some clue to solve the puzzle of SiO maser pumping in late-type and young stellar objects. For this reason, we mapped emission of the SiO $J = 1$–0 $v = 1$ transition in IRC −10414 with the VLBA (Very Large Baseline Array). Based on the mapping result, we discuss a possible link of this object

* Present address: Mizusawa Astrogeodynamics Observatory, National Astronomical Observatory, Mizusawa, Iwate 023-0861.
† Present address: VERA group, National Astronomical Observatory, Mitaka, Tokyo 181-8588.
‡ The VLBA and the VLA are the facilities of the National Radio Astronomy Observatory operated by Associated Universities, Inc., under cooperative agreements with the National Science Foundation of the USA.

Table 1. IRC −10414 observational results (single dish).

	$v=1$ $J=1$–0					$v=2$ $J=1$–0					
Date	T_a^{peak}	V_{lsr}^{peak}	V_{lsr}^{ave}	Int. I.	rms	T_a^{peak}	V_{lsr}^{peak}	V_{lsr}^{ave}	Int. I.	rms	I.I.ratio
(yymmdd)	(K)	(km s^{-1})	(km s^{-1})	(K km s^{-1})	(K)	(K)	(km s^{-1})	(km s^{-1})	(K km s^{-1})	(K)	
970124	13.16	39.51	41.86	58.0	0.32	0.55	40.73	36.70	2.4	0.19	23.8
970217	11.99	39.27	41.62	63.2	0.16	0.76	41.32	40.73	3.6	0.19	17.5
970426	20.27	39.14	41.11	72.3	0.12	0.53	39.29	41.45	1.9	0.14	37.1
980425	4.99	39.88	41.59	36.5	0.22	1.53	40.28	40.99	7.7	0.23	4.6
980606	5.85	36.73	40.02	30.5	0.24	0.70	38.94	53.31	2.7	0.23	10.9
990522	4.89	45.80	43.08	33.6	0.24	0.51	41.87	38.13	1.53	0.07	21.9
	$v=1$ $J=2$–1					$v=2$ $J=2$–1					
990522/23	1.85	39.02	44.82	14.25	0.05	0.21	38.79	40.94	1.19	0.08	12.0

to young stellar objects.

2. Observations

Single-dish observations with the 45-m radio telescope at Nobeyama were made during 1997–1999 in a SiO maser survey of galactic-disk IRAS sources (Izumiura et al. 1999). The object IRC −10414 was used as a pointing check for the 45-m telescope during the survey observations simultaneously by the SiO $J=1$–0 $v=1$ and 2 transitions at 43.122 and 42.821 GHz, respectively. A cooled SIS receiver with a band width of about 0.4 GHz was used, and the system temperature (including atmospheric noise) was about 200–300 K. The aperture efficiency of the telescope was about 0.54 at 43 GHz and the half-power beam width was about 40″ at 43 GHz. The conversion factor from the antenna temperature to the flux density was 3.2 Jy K^{-1}. An acousto-optical spectrometer array of high resolution was used, giving an effective spectral resolution of 0.29 km s^{-1}. Details concerning the observations will be found in Izumiura et al. (1999).

At the middle of 1997, we recognized that the intensity of the SiO $J=1$–0 $v=2$ transition of the pointing source IRC −10414 was unusually weak ($T_a \leq 0.5$ K) compared with the intensity of the $J=1$–0 $v=1$ transition ($T_a \sim 12$ K). A summary of the 1997–1998 observations of IRC −10414 is given in table 1. The data were taken twice every day during a-few-days to one-week sessions of observations in 1997. The daily variation in the line profile of the $J=1$–0 $v=1$ transition was unrecognizable. Therefore we have shown the data taken in one time observation in the session. All of the data of IRC −10414 were taken in the 5-point pointing observation mode. Therefore, the integration was made using only the spectra at the on-source position, and data at the half-beam-off position were abandoned. Linear baseline removal was applied for all spectra. We used the data with low wind velocity (≤ 3 m s^{-1}) when the average pointing accuracy was better than 5″. The daily peak-intensity variation was found to be small (≤ 0.5 K). We have shown only the data with the lowest wind velocity in a session. In 1998, the intensity of the $v=1$ transition became relatively weak ($T_a \simeq 5$ K), but the profile of the $v=2$ transition became recognizable on the baseline. Figure 1 shows the profile change of the SiO $J=1$–0 $v=1$ and 2 in IRC −10414 in 1997–1999. Additional observations were made on 1999 May 22 and 23 to check the intensities of the SiO $J=2$–1 $v=1$ and 2 lines of this star at 86.243 and 85.640 GHz, repectively. An acousto-optical spectrometer having a low resolution was used (giving a velocity resolution of 0.87 km s^{-1} at 86 GHz) for the $J=2$–1 lines. The $J=2$–1 $v=2$ line was marginally detected (≤ 0.2 K), although strong emission of the $J=2-1$ $v=1$ line was seen ($T_a^{peak}=1.8$ K; 6.5 Jy). Profiles for the $J=2$–1 lines are shown in the last pannel of figure 1 and line parameters in table 1.

A VLBA observation of the IRC −10414 SiO maser was made at 12:30–18:30 UT on 1998 February 23 with 10 antennas of the VLBA and the single antenna of the Very Large Array (VLA) in a dual circular polarization mode. The 4-MHz band width was used to be centered at $V_{lsr}=42$ km s^{-1}. In the observation, 13–18 min scans were interleaved with 4-min scans of a nearby clock-parameter calibrator, NRAO 530, and a polarization calibrator, OT 081. The data were correlated by the Socorro FX correlator with cross-polarization mode. The VLA position of IRC −10414 ($18^h20^m27^s.82$, $-13°44'24''.1$ for the OH maser at the epoch of 1950; Blommaert et al. 1994) was chosen as a source position. The velocity spacing of each spectral channel was 0.22 km s^{-1}.

Calibration of the visibility data was performed in the

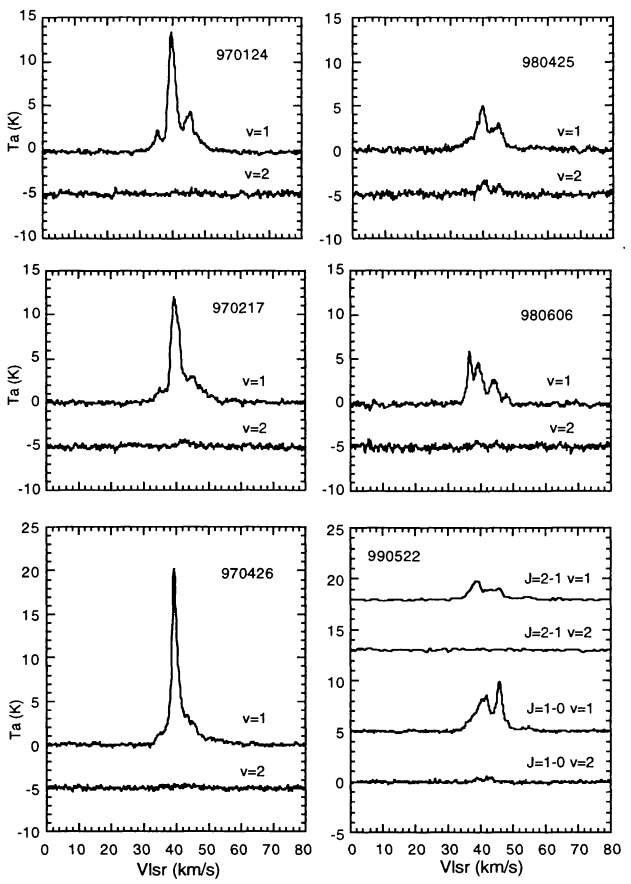

Fig. 1. Time variation of the spectra of the SiO $J = 1$–0 $v = 1$ and 2 lines in IRC −10414. Observed date are shown on the upper right corner in each panel in the yymmdd format. The $J = 1$–0 $v = 2$ line was quite weak in 1997 but was recognizable in 1998. The last pannel shows the profiles of the $J = 2$–1 $v = 1$ and 2 lines.

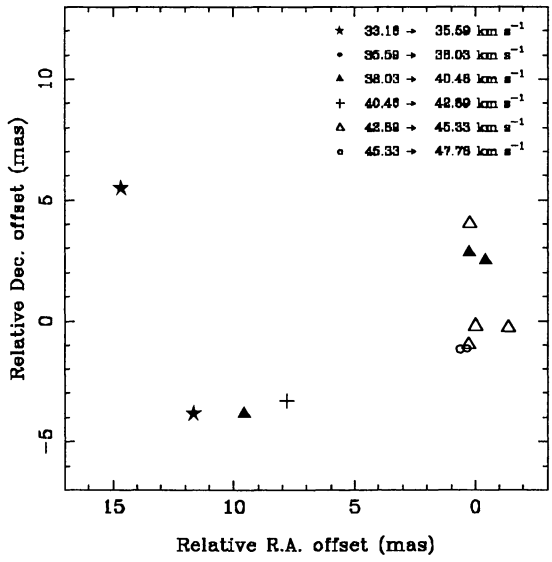

Fig. 2. Map of the SiO $J = 1$–0 $v = 1$ emission in IRC −10414.

NRAO AIPS package. For this paper, we used only the data of a parallel circular correlation. An amplitude calibration was accomplished using recorded system temperatures (80–300 K) and tabulated values for the antenna gains at 43 GHz (0.030–0.098 K Jy^{-1}). After calibrating for station clock offsets and clock-rate offsets using the data of NRAO 530, calibration for fringe-rates was performed using strong maser emission on the velocity channel at 45.04 km s^{-1}. Self-calibration for the visibility amplitudes and phases were performed on the velocity channel at 45.04 km s^{-1}. A solution interval of 24 s was chosen to assure an adequate signal-to-noise ratio and to avoid any decorrelation effect of the atmosphere. The uncertainty of the absolute amplitude scale comes from the uncertainty of the antenna gains (20%; e.g., Greenhill et al. 1995). The resulting amplitude/phase corrections were applied to the entire velocity channels with maser emission.

The final synthesis images for the SiO masers were obtained by the CLEAN deconvolution technique using the AIPS. The FWHM width and position angle of the synthesized beam were 0.80 × 0.45 mas and −1°, respectively, in natural weighting. The obtained image cubes consisted of individual channel maps with a field size of about 40 mas × 40 mas between −50 km s^{-1} and −30 km s^{-1}. The data near to the band edges were not available because of including strong phase-calibration tones and low sensitivity.

We determined the parameters of the individual maser feature, consisting of a cluster of maser spots in the same position within 1 mas, by quadratic fitting for the peak intensities with respect to the velocities near to the most intense maser spot. The obtained quantities of the detected features (relative positions, peak intensities, and velocity width) are given in table 2.

Figure 2 shows the map of maser spots of the SiO $J = 1$–0 $v = 1$ transitions in IRC −10414. The map exibits a tendency that the lower velocity components (the filled marks) are concentrated on the left and the higher velocity components (unfilled) are on the right of the map. The average velocity gradient in the east–west direction is about −0.7 km s^{-1} mas^{-1}. Table 2 summarizes the observed quantities of the detected components: positions, peak intensities, and velocity widths. Because the components at 44.935 km s^{-1} were used for the phase-

Table 2. Parameters of detected SiO maser features around IRC −10414.

V_{lsr}*	Relative R.A. offset†	R.A. offset error	Relative Dec. offset†	Dec. offset error	Peak intensity	Velocity width‡
(km s^{-1})	(mas)	(mas)	(mas)	(mas)	(Jy/beam)	(km s^{-1})
47.763	0.3315	0.0440	−1.1519	0.0292	0.560	2.176
46.048	0.6042	0.0444	−1.1638	0.0242	0.544	0.652
44.414	0.2769	0.0521	−1.0119	0.1189	1.149	2.073
44.935§	0.0003	0.0915	−0.2246	0.0451	2.605	3.096
43.949	−1.3663	0.0271	−0.3048	0.0381	0.754	1.632
43.819	0.2236	0.0315	4.0006	0.0256	1.323	1.967
42.009	7.8179	0.0188	−3.3155	0.0361	0.692	2.188
39.980	−0.4285	0.0365	2.4645	0.0712	1.455	2.587
38.637	9.5667	0.0447	−3.8656	0.0649	1.077	2.380
39.695	0.2151	0.0367	2.8136	0.0638	0.557	2.103
35.259	11.6269	0.0238	−3.8502	0.0275	0.676	1.206
33.157	14.6448	0.1060	5.4601	0.1863	0.604	3.027

*Fitted intensity-peak velocity of maser feature.
†Fitted intensity-peak position at the epoch of the observation.
‡Fitted full width at half power of the peak intensity.
§Velocity channel used for phase-referencing.

referencing, the origin of the coordinates was shifted to the west in this map. The positional errors are less than 0.1 mas for most of the maser spots. The total integrated flux of the detected components is 27.5 Jy km s^{-1}, which is about one third of the flux measured by the 45-m telescope on 1998 April 25. The correlated flux by the VLBA is probably about one third of the flux observed by the single-dish telescope.

3. Discussion

3.1. *Circular and Rotating Ring Models*

The distance to IRC −10414 was deduced to be about 710 pc (Jura, Kleinman 1989), giving 1 mas as 1.1×10^{13} cm. The thin broken curve in figure 3 is an approximate fit of the spot positions with a circle. The radius of the circle corresponds to 1.6×10^{14} cm. This is consistent with the fact that the SiO masers are emitted in the region of 2–4 stellar radii (Diamond 1994) when the radius of the photosphere of this type of stars is $\sim 6 \times 10^{13}$ cm (assuming $T_{\rm photosphere} = 2000$ K and $L = 10^4 L_\odot$). This is consistent with the picture that SiO masers are emitted from the periphery of the photosphere and in a direction almost tangential to the radial expansion. In this case, the central star is probably located at the center of the circle.

Figure 2 exhibits a velocity gradient of 0.7 km s^{-1} mas^{-1} in the east–west direction. It is possible to interpret the origin of the velocity field as being due to the expanding/contracting rotating disk or ring. The thick broken curve in figure 3 shows a least-squares fit by the rotating contracting ring model. Table 3 summarizes the

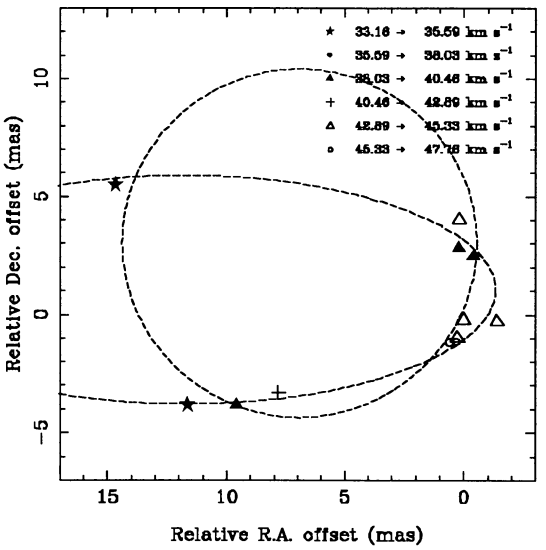

Fig. 3. Overlay of the rotating ring on the SiO $J = 1$–0 $v = 1$ map. The broken circle shows the fit by the standard expansion model and the broken ellipse the fit by the rotating ring model.

Table 3. Parameters of a rotating ring model.

Parameter	Value		Standard error
Diameter	26.3	±	3.8 mas†
x_0*	11.5	±	2.2 mas
y_0*	0.8	±	1.1 mas
Inclination	110.5	±	6.°8
Position angle	2.4	±	9.°5
$V_{\rm rotation}$‡	12.2	±	1.4 km s^{-1}
$V_{\rm expansion}$§	−3.3	±	1.6 km s^{-1}
$V_{\rm systemic}$¶	34.1	±	1.0 km s^{-1}

*Position of the center of the disk model.
†Error is defined by $\Delta\chi^2 < 1$.
‡Rotation velocity of the rotating ring model.
§Expansion velocity of the rotating ring model.
¶Systemic velocity of the rotating ring model.

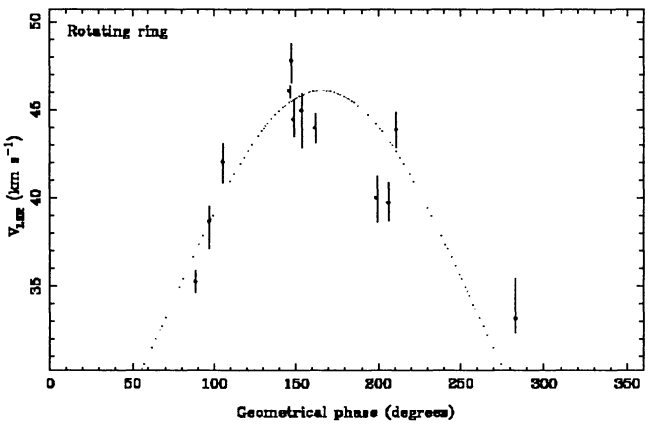

Fig. 4. Plot of the radial velocity against geometrical phase in a rotating ring model. The dotted curve is the sine curve with period of 2π.

model parameters for the best-fit ring. A systemic velocity of 34.6 km s^{-1} and a rotation velocity of 11.6 km s^{-1} at the radius of 13.1 mas (1.39×10^{14} cm) were obtained. The contracting speed, −2.9 km s^{-1}, seems to be insignificant and not very different from zero. Contraction is necessary to fit the feature of a north–south velocity gradient on the spot complex at the right side of the figure. Figure 4 shows a plot of the radial velocity against the geometrical phase of the ring position. The ring center should be at (11.5 mas, 0.8 mas) on this map. If the ring is gravitationally bound to the central star, the position of the central star must coincide with the disk center. Neglecting the contracting motion, we can derive the mass of the central star (assuming the Keplerian motion) as $1.4\,M_\odot$. The rotation period of the ring is about 23 years.

The OH 1612 MHz double peaks in IRC −10414 appear at $V_{\rm lsr}$ = 27.3 and 59.1 km s^{-1} (Blommaert et al. 1994), giving a systemic (stellar) velocity of 43.2 km s^{-1}. The spectra of OH 1612 MHz which were taken by Ukita and Goldsmith (1984) exhibited a complex profile of the higher and lower velocity components splitting into severals. It seems difficult to obtain an accurate systemic velocity with applying a simple doublely-peaked-profile picture to this source. The intensity-averaged radial velocity of SiO maser spots in the VLBA observation in the present paper is 42.2 km s^{-1}, which is consistent with the systemic velocities derived from OH 1612 MHz by Blommaert et al. (1994). Observations of H_2O (Kleinman et al. 1978) give 29–44.5 and SiO masers (Ukita, Goldsmith 1984) 37 km s^{-1}. However, Blommaert et al. (1994) noted that there is a disagreement in the reference: ∼20 km s^{-1} (SiO $J = 1$–0 $v = 1$; Barcia et al. 1985). From these facts, we consider that the systemic velocity of this star is probably in the range 37–42 km s^{-1}.

The systemic velocity derived from the rotating-ring model, 34.6 km s^{-1}, is not totally inconsistent with above systemic velocity derived from OH 1612 MHz and H_2O/SiO observations. However, the difference in the systemic velocity derived by the rotating ring model seems to be a bit large if we take the value 43 km s^{-1}, derived from OH 1612 MHz observation by Blommaert et al. (1994). This seems to suggest that the simple-minded rotating-ring model cannot explain the velocity field of the observed spots.

It is possible that the radial velocities of the spots are produced simply by spherically symmetric expansion of the envelope, in which the spots are fragments of gas. The random distribution of the maser spots may produce, by chance, a velocity-gradient feature. In fact, VLBI maps of maser spots in many other stars in the SiO $J = 1$–0 $v = 1$ line exhibit similar levels of velocity gradient (for example, VX Sgr; Miyoshi et al. 1992; Greenhill et al. 1996). However, we have to note that the VLBA mapping provided the positions of strong maser spots which contain only one third of the total SiO maser flux. The maser spots which have been observed by the VLBA may be somewhat biased in intensity, and appreciable numbers of components are resolved out. The multi-epoch observations are absolutely required to confirm this issue.

3.2. *Speculation on the Line Intensity Ratio*

The transitions of the SiO $J = 1$–0 $v = 1$ and 2 lines lies at approximately 1785 and 3570 K, respectively, from the ground level. It is natural to consider that only one of maser transitions in the $v = 1$ or 2 vibrational state is

activated at one position in the envelope. Then the differences in the physical conditions between the $v = 1$ and 2 masers should lead a large intensity difference between two maser transitions. However, in reality, the ratio is nearly unity in many late-type stars. The VLBI observations of the $J = 1$–0 $v = 1$ and $v = 2$ transitions in the normal late-type stars have shown that maser emissions in both transitions come from almost the same spots in the envelope (Miyoshi et al. 1992).

It has been suggested that the intensity ratio of about unity of the two transitions of SiO is due to line overlap of the SiO $(J = 0\ v = 1)$–$(J = 1\ v = 2)$ transition (2–1 R0) with the H_2O vibration–rotation line ($\nu_2 = 0\ 12_{73} \rightarrow \nu_2 = 1\ 11_{66}$; Miyoshi et al. 1992). This line overlap was originally proposed by Snyder and Buhl (1975) to explain the weakness of the $J = 2$–1 $v = 2$ maser. The pump cycle in the SiO energy levels ($J = 0\ v = 1 \Rightarrow J = 1\ v = 2 \rightarrow J = 0\ v = 2 \Rightarrow J = 1\ v = 1 \rightarrow J = 0\ v = 1$) can produce the same number of photons in the $J = 1$–0 $v = 1$ and 2 transitions when both masers are saturated. Here, the transition ($J = 0\ v = 1 \Rightarrow J = 1\ v = 2$) is pumped by the H_2O vibration-rotation transition and the transition ($J = 0\ v = 2 \Rightarrow J = 1\ v = 1$) occurs due to a radiative escape. Oloffson et al. (1985), Bujarrabal et al. (1996), and Cho et al. (1998) investigated this further and found that a clear trend favoring emission from the SiO J =2–1 $v = 2$ line in S type stars which are deficient in H_2O. The frequency difference between the SiO R0 ($v = 1$) transition ($J = 0\ v = 1 \Rightarrow J = 1\ v = 2$) of the H_2O vibration-rotation line is known to coincide within ~ 0.004 cm^{-1} (about $\sim$1 km s^{-1}) (Bujarrabal et al. 1996).

If this mechanism is a correct explanation, the weakness of the $J = 1$–0 $v = 2$ line in IRC −10414 is due to either of the two reasons: (1) the H_2O vapor is deficient in the envelope of IRC −10414, or the water vapor content is time variable, and (2) the excitation temparature of the overlapped water line is significantly lower than the excitation temperature of the SiO vibrational lines. Detections of water maser emission in IRC −10414 and other young stellar objects seem to exclude reason (1). Bujarrabal et al. (1996) calculated the excitation of the H_2O and SiO lines by applying the overlap with the quenching of the SiO $J = 2$–1 $v = 2$ line. In this calculation with the H_2O line overlap, the $J = 2$–1 $v = 2$ maser occurs when $T_{ex}(H_2O) < T_{ex}(SiO)$, where the line overlap works as a photon sink through the $J = 1$ $v = 2$ level for the J =2–1 maser. In this case, the $v = 2$ $J = 1$–0 maser is quenched. Because the H_2O vibrational lines are more optically thick than SiO vibrational lines especially in low density (as $n_{H_2} < 5 \times 10^9$ cm^{-3} ; Bujarabal et al. 1996), the excitation temperatures of H_2O lines are higher than those of SiO lines. The subtle difference of the excitation temepartures of the relevant 8 μm H_2O and SiO lines in the envelope can cause a quenching of the $J = 1$–0 $v = 2$ line. The geometry of the envelope (possibly a thin rotating disk) may help the escape of H_2O line photons from the surface of the disk and lower the excitation temperature of the H_2O lines. In such a case, it is possible to quench the SiO $J = 1$–0 $v = 2$ maser with this line overlap. However, the failure of the simple rotating-ring model, described in the previous section, seems to exclude this case. Also, a SiO source such as Orion IRC2, which has a disk structure (Plambeck et al. 1990), exbibits almost an equal intensity ratio of the $v = 1$ to 2 line.

The weakness of the $J = 2$–1 $v = 2$ line in IRC −10414 in 1999 May (section 2) produces another puzzel for interpretation; the quenching may be made without the H_2O line overlap, suggesting an effect due to a high density or a low kinetic temperature in the envelope. Though there is stil space to play a model with a complex structure in the envelope (for example see Bujarrabal et al. 1996), the line-ratio problem of the SiO $v = 1$ and 2 maser lines seems to remain unsolved.

4. Conclusion

We observed IRC −10414 with the VLBA in the SiO $J = 1$–0 v=1 transition. In this source, a single-dish observation has shown that the line intensity ratio of the SiO J=1–0 $v = 1$ to $v = 2$ transition is unusually large. Though the obtained VLBA map with a spatial resolution of better than 0.1 mas exhibits a velocity gradient in the east-west direction, it is difficult to interpret the spatial distribution and radial velocities of the maser spots using a simple, expanding/contracting-rotating-ring model.

The authors would like to thank the staff of NRAO for the assistance of VLBA observations. They also thank to Dr. H. Izumiura and Mr. J. Nakashima for letting us use the pointing data taken by the 45-m telescope and for the help of data reduction, and Dr. V. Bujarrabal for comments. H.I. is financially supported by the Research Fellowship of the Japan Society for the Promotion of Science for Young Scientist. This work was supported by Grant-in-Aid of Ministry of Education, Science, Sports and Culture (c) No. 10640238.

References

Barcia A., Bujarrabal V., Gómez-Gónzalez J., Martin-Pintado J., Planesas P. 1985, A&A 142, L9

Blommaert J.A.D.L., Van Langevelde H.J., Michiels W.F.P. 1994, A&A 287, 479

Bujarrabal V., Alcolea J., Sanchez Contreras C., Colomer F. 1996, A&A 314, 883

Cho S.-H., Chung H.-S., Kim H.-R., Oh B.-Y., Lee C.-H., Han

S.-T. 1998, ApJS 115, 277
Diamond P.J., Kemball A.J., Junor W., Zensus A., Benson J., Dhawan V. 1994, ApJ 430, L61
Engels D. 1979, A&AS 36, 337
Fuente A., Martín-Pintado J., Alcolea J., Barcia A. 1989, A&A 223, 321
Greenhill L.J., Colomer F., Moran J.M., Backer D.C., Danchi W.C., Bester M. 1995, ApJ 449, 365
Hasegawa T., Morita K.-I., Okumura S., Kaifu N., Suzuki H., Ohishi M., Hayashi M., Ukita N. 1985, in Masers, Molecules, and Mass Outflows in Star Forming Region, ed A.D. Haschick (Haystack Observatory)
Izumiura H., Deguchi S., Fujii T., Kameya O., Nakada Y., Ootsubo T., Ukita N. 1999, ApJS in press
Jiang B.W., Deguchi S., Izumiura H., Nakada Y., Yamamura I. 1995, PASJ 47, 815
Jura M., Kleinmann S.G. 1989, ApJ 341, 359
Kleinmann S.G., Dickinson D.F., Sargent D.G. 1978, AJ 83, 1206
Lockwood G.W. 1985, ApJS 58, 167
Miyoshi M., Morimoto M., Kawaguchi N., Ukita N., Inoue M., Miyazawa K., Tsuboi M., Miyaji T. et al. 1992, Nature 371, 395
Morita K.I., Hasegawa T., Ukita N., Okumura S., Ishiguro M. 1992, PASJ 44, 373
Nakada Y., Onaka T., Yamamura I., Deguchi S., Ukita N., Izumiura H. 1993, PASJ 45, 179
Nyman L.-Å., Olofsson H. 1986, A&A 158, 67
Olofsson H., Rydbeck O.E.H., Nyman L.-Å. 1985, A&A 150, 169
Plambeck R.L., Wright M.C.H., Carlstrom J.E. 1990, ApJ 348, L65
Schwartz P.R., Waak J.A., Bologna J.M. 1979, AJ 84, 1349
Shiki S., Ohishi M., Deguchi S. 1997, ApJ 478, 206
Snyder L.E., Buhl D. 1975, ApJ 197, 329
Spencer J.H., Winnberg A., Olnon F.M., Schwartz P.R., Matthews H.E., Downes D. 1981, AJ 86, 392
Ukita N., Goldsmith P.F. 1984, A&A 138, 194